Available online at www.sciencedirect.com
ScienceDirect
Journal of Fluorine Chemistry 128 (2007) 839–843
JOURNAL OF FLUORINE CHEMISTRY
www.elsevier.com/locate/fluor

A crystalline H-bond cluster of hexafluoroisopropanol (HFIP) and piperidine
Structure determination by X ray diffraction

J.-F. Berrien [a], M. Ourévitch [a], G. Morgant [a], N.E. Ghermani [b], B. Crousse [a], D. Bonnet-Delpon [a,*]

[a] *BioCIS, UMR CNRS 8076, IFR 141, Faculté de Pharmacie Univ. Paris-Sud, 5 rue J.B. Clément, 92296 Châtenay-Malabry, France*
[b] *Laboratoire PPB, UMR CNRS 8612, IFR 141, Faculté de Pharmacie Univ. Paris-Sud, 5 rue J.B. Clément, 92296 Châtenay-Malabry, France*

Received 21 February 2007; received in revised form 12 March 2007; accepted 13 March 2007
Available online 24 March 2007

Abstract

Piperidine and 1,1,1-3,3,3 hexafluoro-2-propanol (HFIP) have been co-crystallized and X-ray crystal structure has been explored. Single-crystal X-ray analysis displays the existence of hydrogen bonding aggregates through dimers **1** of the complex (one piperidine/two HFIP) where the heteroatoms form a six-center ring. In this cluster **1**, each heteroatom (N, O) is multiple H-bond donor and acceptor. Surprisingly the strongest H-bond of the network is where HFIP acts as an acceptor from the amine. In this complex HFIP adopts a conformation different from that of HFIP aggregates. The supramolecular architecture is also based on discrimination between polar and hydrophobic parts that allows the alignment of molecules and the formation of parallel channels. NMR experiments show that strong interactions between piperidine and HFIP are maintained in solution.

Keywords: Fluorinated alcohol; H-bond; Self-association; X-ray structure

1. Introduction

Fluorinated alcohols like trifluoroethanol (TFE) or hexafluoroisopropanol (HFIP) are polar protic solvents with high ionizing power. They display poor nucleophilicity and high acidity, and they are strong H-bond donors ($\alpha = 1.51$ and 1.96 respectively) [1], but very poor H-bond acceptors ($\beta = 0$). When used as solvents, their properties facilitate clean and selective reactions [2]. For example, HFIP activates oxirane ring opening with poorly nucleophilic aromatic amines. In contrast, more nucleophilic aliphatic amines like piperidine did not react with epoxides under the same conditions [3]. In this latter case, it was postulated that HFIP formed an association with nucleophilic amines, resulting in both a deactivation of amines and a decreased catalytic activity of HFIP. Fluorinated alcohols are effectively known to form stable H-bonded complexes with Lewis bases [4]. Most of these complexes have been studied in solution by IR, Raman and NMR techniques, by enthalpy measurements and by molecular modeling [5]. Furthermore, fluoroalcohols and fluoroalcohol-containing molecules have been reported to form self-aggregates through hydrogen bonding [4b–6]. Some of these structures have been studied by X-ray spectroscopy. We report herein the co-crystallization, at room temperature, of HFIP and piperidine, and a study on the structural feature of the formed hydrogen bonding supramolecular edifice.

2. Results and discussion

Mixing HFIP ($pK_a = 9.3$) and piperidine ($pK_a = 11.1$) which are both liquid at room temperature (m.p. = −4 and −10 °C, respectively), resulted in a precipitate. This solid was recrystallized in toluene leading to colorless crystals (m.p. = 95 °C). The architecture of the crystal, determined by single-crystal X-ray diffraction, is formed of supramolecular assemblies of six-center chair-like cycles involving two molecules of piperidine

* Corresponding author.
E-mail address: Daniele.Bonnet-Delpon@cep.u-psud.fr (D. Bonnet-Delpon).

0022-1139/$ – see front matter © 2007 Elsevier B.V. All rights reserved.
doi:10.1016/j.jfluchem.2007.03.014

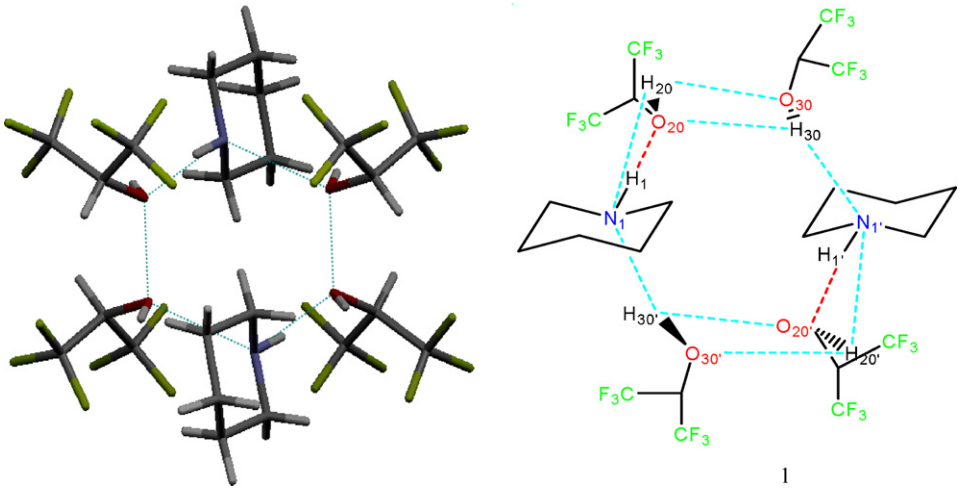

Fig. 1. Detailed structure of cluster **1**.

and four molecules of HFIP (Fig. 1). The cohesion is the result of cooperative multiple hydrogen bonds. The lattice is composed of one molecule of piperidine and two non-equivalent molecules of HFIP, confirming thus theoretical studies reported for 1-methylindole and HFIP interactions [5b]. Clusters **1** stack with each other along the unit-cell axis to form infinite parallel channels (Fig. 2).

2.1. Description of the lattice

The excellent resolution of X-ray structure (residual factor = 0.0366) allowed an unambiguous location of all hydrogen atoms. Although a major H-bond between HFIP as donor and piperidine as acceptor was highly expected, the hydrogen bond system exhibited unexpected specific features. In the lattice, the two molecules of HFIP are not equivalent. The hydroxyl group of the first molecule of HFIP participates in four H-bonds. It is donor to and acceptor from the NH of piperidine (H_{20}–N_1 = 2.39 Å, O_{20}–H_1 = 1.71 Å). It is also donor to and acceptor from the hydroxyl of the second molecule of HFIP (H_{20}–O_{30} = 2.50 Å, H_{30}–O_{20} = 2.53 Å) (Table 1). Similarly piperidine is both H-bond donor and acceptor. The second molecule of HFIP interacts with the first one as donor and acceptor. In these interactions, the system exhibits single-proton four-center hydrogen bonds. Such multi-center hydrogen bonds are known to be 0.2 Å average longer than classical two-center H-bond [7].

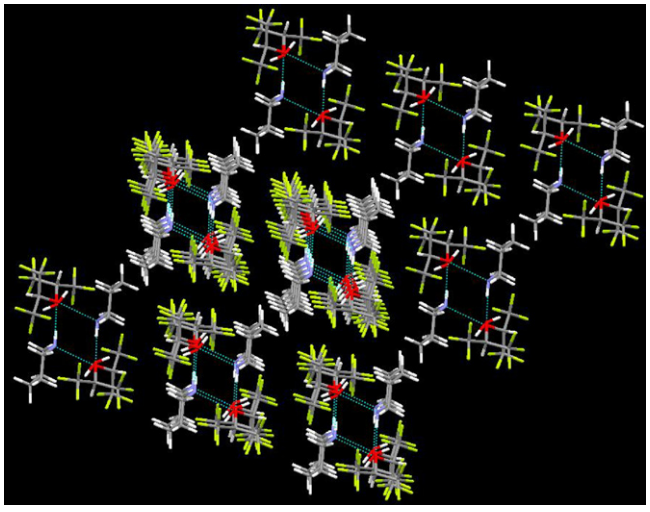

Fig. 2. Packing diagram of crystal **1**.

All interaction distances are shorter than the sum of van der Waals nuclei. However the H-bond O_{20}–$H_{20}\cdots N_1$, which corresponds to the expected donor ability of HFIP, is not a strong one (d = 2.39 Å, ∠ = 94.5°). This rules out a classical alkoxide/ammonium zwitterionic association, that have been previously observed for crystalline trifluoromethyl amino alcohols [5g]. The presence of multi-center H-bonds indicates that the cohesion of the system is due to a more sophisticated association. Cooperative aggregation not only leads to enhanced H-bond donor ability but also to H-bond acceptor ability for all heteroatoms. Moreover the strongest H-bond, in terms of distance and of angle, is N_1–$H_1\cdots O_{20}$ (d = 1.71 Å, ∠ = 164.3°), where HFIP is an acceptor and the secondary amine a donor. This surprising H-bond with a distance of 2.58 Å between both heteroatoms is expected to be highly stabilizing [8].

The cohesion of the homodimeric complex of piperidine/$(HFIP)_2$ is essentially due to both hydrogen bonds $N_1\cdots H_{30'}$ and $N_{1'}\cdots H_{30}$ (2.71 Å, H_1–$N_1\cdots H_{30'}$ = 126.9°) where nitrogen acts as an H-bond acceptor.

2.2. HFIP in the cluster *1*

The two alcohol functions are head-to-tail bonded in a quasi-planar four-center system. This arrangement maximizes

Table 1
H-bond donor/acceptor (DHA) for $C_{11}H_{15}F_{12}N_1O_2$

	d (Å)	∠(DHA) (°)
$H_{20}\cdots N_1$	2.39	O_{20}–H_{20}–N_1 = 94.5
$O_{20}\cdots H_1$	1.71	O_{20}–H_1–N_1 = 164.3
$H_{20}\cdots O_{30}$	2.50	O_{20}-H_{20}-O_{30} = 70.0
$H_{30}\cdots O_{20}$	2.53	O_{20}–H_{30}–O_{30} = 67.9

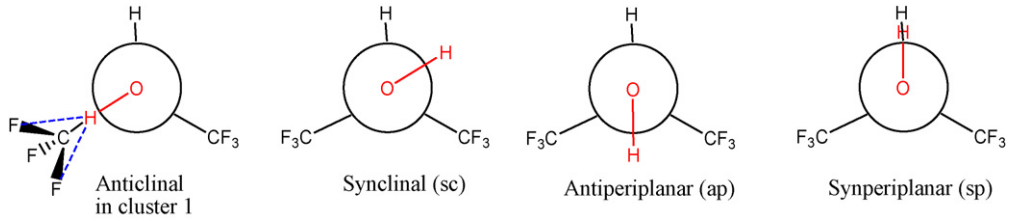

Fig. 3. Different conformations of HFIP in cluster **1** and in self-aggregation.

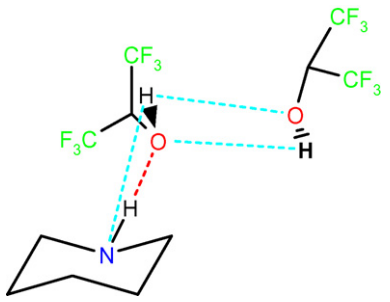

Fig. 4. Canonical representation of $C_{11}H_{15}F_{12}N_1O_2$.

dipole–dipole interactions and reflects the strongly polarized OH bond of HFIP [9].

The conformation of HFIP in cluster **1** has been compared to that of HFIP in solution and HFIP in self-aggregation (Fig. 3). Earlier Raman and IR studies characterized the existence of synclinal (sc, angle torsion around + −60°) and antiperiplanar (ap, angle torsion around + −180°) conformers in the gas phase or in solutions [10]. Furthermore, recent crystallographic studies [4b] show that, upon aggregation, the dihedral angle Hc–C–O–H is around 30° indicating a synclinal conformation close to a synperiplanar (sp) one. These conformations have been claimed to be a characteristic of HFIP as hydrogen bond donor [4b].

In the cluster **1**, the conformation of both molecules of HFIP is anticlinal (ac), where Hc–C–O–H = 100°. OH bonds are eclipsed with one of the two C–CF_3 bonds. To our knowledge, there is no report on such anticlinal characterized conformation of HFIP. This geometry implies a proximity between the hydroxyl proton and fluorine atoms. Indeed, two $OH_{20}\cdots F$ distances are around 2.50 Å and two $OH_{30}\cdots F$ distances are only 2.37 Å, which can be considered as tight interactions. However, this is unlikely to be a driving force for the formation of the network since such intramolecular F···H-bonds are not reported in aggregates of HFIP. No other short F···H distances have been found in the cluster (Figs. 4 and 5).

It is worth noting that HFIP alone shows broad strong OH stretching band in the liquid phase (3430 cm^{-1}) or in the solid phase (3260 cm^{-1}) [11] while, in the cluster **1**, this band appears at lower frequency (∼3000 cm^{-1}).

2.3. Characteristic of the supramolecular association

Hydrophobic parts of HFIP and piperidine molecules are located outside of the cluster **1** and are in contact in the

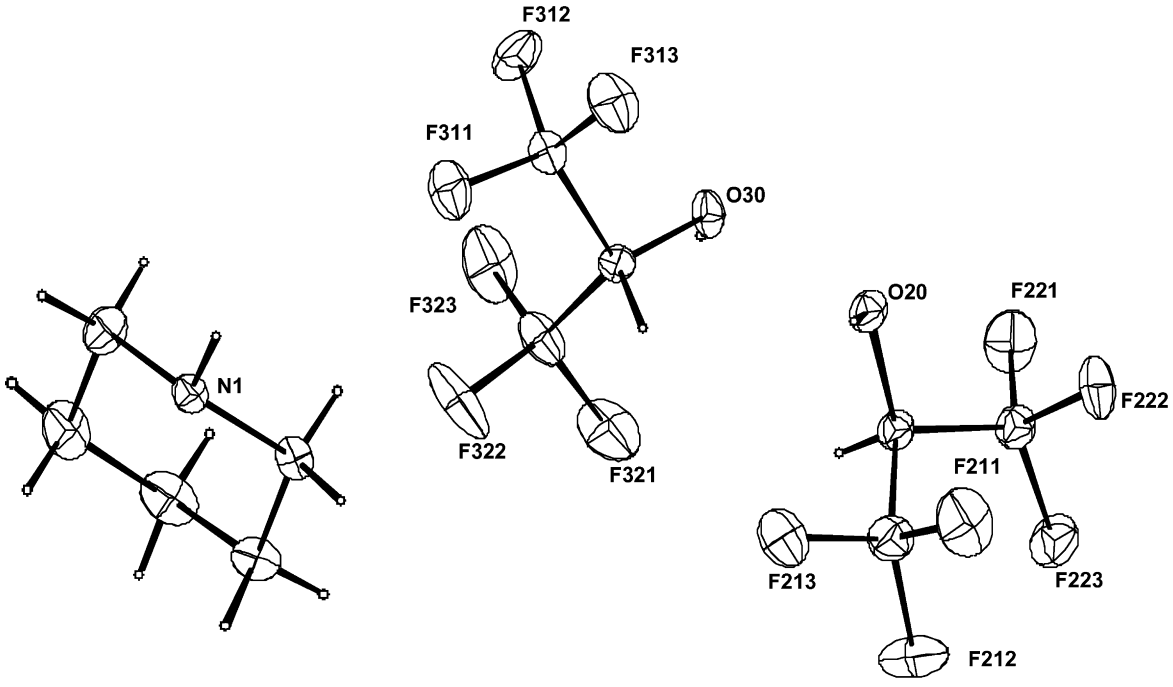

Fig. 5. Labelled CAMERON [16] diagram of $C_{11}H_{15}F_{12}N_1O_2$. Ellipsoids are drawn at 50% probability level.

crystal with corresponding hydrophobic groups of neighboring clusters. Spatial arrangement of clusters in the crystal segregates contacts between fluorinated groups and alkyl chains (microphase separation). This clearly evidences the low affinity existing between the trifluoromethyl groups of HFIP and the CH_2 groups of piperidine. The same holds for the packing into layers. In contrast, in H-bond clusters of HFIP–water, NMR data suggested a micellar structure with the hydrophobic CF_3 groups located in the inside core of the micelle, and hydrophilic OH groups in the outside shell to form H-bond with surrounding water [12]. In case the generation of cluster **1** could be dependent on solvent, we have performed crystallization of piperidine/HFIP from hot water. Produced crystals have the same 95 °C melting point and the same IR spectrum than crystals obtained from toluene.

2.4. NMR data

^{1}H NMR of the cluster **1** in $CDCl_3$ solution could not differentiate the two molecules of HFIP. Both NH and OH functions gave a single signal which is concentration dependent and is strongly deshielded at saturation (10 mg mL^{-1}, 6.09 ppm) compared with HFIP alone (3.15 ppm). In more diluted solution (1 mg mL^{-1}) this signal was shielded at 1.26 ppm. Piperidine CH_2 signals are deshielded about 0.1 ppm and are concentration independent. ^{19}F NMR gave only one doublet. HOESY experiment (^{1}H, ^{19}F) at 10 mg mL^{-1} in $CDCl_3$ showed the proximity of fluorine atoms to the CH_2 of piperidine, with a stronger correlation for the protons in α position of the nitrogen. This indicates that piperidine and HFIP are still H-bonded in $CDCl_3$. This HOESY effect disappeared in CD_3OD or DMSO-D6, H-bonds between piperidine and HFIP likely being broken in these solvents.

3. Conclusions

The most important of our study can be summarized as follows.

Self-assembly through multiple and strong H-bonds of piperidine and HFIP resulted in a crystalline co-polymer. The high cohesion of the crystal is demonstrated by its thermal stability (m.p. = 95 °C) while individual components are liquid at room temperature. The lattice is a one piperidine/two HFIP complex which dimerizes to form the cluster **1**. The overall hydrogen bonding system is typically formed of single-proton, multi-center bondings. The more striking and unexpected result is that, in this network, HFIP undergoes the strongest hydrogen bond as an acceptor and not as a donor. The supramolecular architecture is also based on a discrimination between polar and hydrophobic parts which allows an alignment of molecules through different microphases. Changes in OH-bond polarization, along with the modification of HFIP conformation in the cluster **1**, compared to that of aggregate of HFIP alone, are expected to bring specific properties.

4. Experimental

4.1. NMR data

Cluster **1**: m.p. 95 °C (sublimate). IR (neat); ν 3038, 2958, 2872, 2752, 2649, 2542, 2447, 1624, 1376, 1162, 1087, 887, 684; ^{13}C NMR (50 MHz, $CDC1_3$) 23.7 (C-4), 25.0 (C-3, C-5), 45.8 (C-2, C-6), 69.7 (septet, J = 32.6 Hz, C-20, C-30), 122.4 (q, J = 284.8 Hz, CF3). ^{1}H NMR (200 MHz, $CDCl_3$): 1.65–1.85 (m, 6H, H-3 H-4 and H-5), 2.85-3.05 (m, 4H, H-2 and H-6), 4.43 (septuplet, 2H, J = 6.5 Hz, H-201, H-301), 6.05–6.25 (bs, 3H, H-1, H-20, H-30). ^{19}F NMR (100 MHz, $CDC1_3$): −76.17 (d, 12F, J = 6.5 Hz). Anal. Calcd for $C_{11}H_{15}F_{12}NO_2$: C, 31.3; H, 3.6; N, 3.3. Found: C, 31.5; H, 3.7; N, 3.3.

4.2. X-ray diffraction study

Diffraction data were collected on a Bruker-SMART three-axis diffractometer equipped with a SMART 1000 CCD area detector using graphite monochromated Mo Kα X-radiation (wavelength λ = 0.71073 Å) at 100 K. The low temperature was reached by an evaporated liquid nitrogen stream over the crystal, provided by the Oxford Cryosystem device. Data collection and processing were carried out using Bruker SMART programs [13] and empirical absorption correction was applied using SADABS computer program [13]. The structure was solved by direct methods SIR97 [14], and refined

Table 2
Crystal data and structure refinement parameters for $C_{11}H_{15}F_{12}N_1O_2$

Compound	$C_{11}H_{15}F_{12}N_1O_2$
Empirical formula	$C_{11}H_{15}F_{12}N_1O_2$
Molecular weight	421.22
Color	Colorless
Crystal system	Triclinic
Space group	*P*-1
a (Å)	9.3645(5)
b (Å)	9.7640(5)
c (Å)	10.4175(6)
α (°)	92.097(1)
β (°)	113.529(1)
γ (°)	108.352(1)
V (Å^3)	814.37(8)
Z	2
Calculated density (g cm^{-3})	1.718
Absorption coefficient (mm^{-1})	0.206
F (0 0 0)	424
Crystal size (mm^3)	0.30 × 0.40 × 0.60
θ ranges (°)	2.17–33.92
h/*k*/*l*	−13, 11/−13, 13/1, 14
T (K)	100(2)
Nb of reflections collected	6070
Nb of independent reflections	4266
Nb of reflections used ≥2 *σ*(I)	2248
Parameters	235
R [F]	0.0366
Wr [F]	0.0428
Goodness-of-fit on *F*	1.1064
Residual density (e Å^{-3})	−0.49, 0.53
Refine is. shift/su.max	0.00036

Table 3
Selected bond distances (Å) and bond angles (°) for $C_{11}H_{15}F_{12}N_1O_2$

Bonds (Å)		Angles (°)		Angles (°)	
F211–C21	1.202(3)	C2–N1–C6	115.97(16)	F223–C22–F221	110.97(17)
F212–C21	1.447(3)	N1–C2–C3	116.37(16)	F223–C22–F222	108.78(17)
F213–C21	1.353(3)	C2–C3–C4	101.12(18)	F221–C22–F222	100.08(18)
F221–C22	1.316(3)	C3–C4–C5	113.78(18)	O30–C30–C31	108.06(15)
F222–C22	1.220(2)	C4–C5–C6	117.77(18)	O30–C30–C32	109.99(16)
F223–C22	1.452(3)	C5–C6–N1	99.60(17)	C31–C30–C32	116.18(16)
F311–C31	1.335(2)	O20–C20–C21	114.53(16)	C30–C32–F322	113.91(18)
F312–C31	1.322(2)	O20–C20–C22	112.09(15)	C30–C32–F323	104.00(19)
F313–C31	1.235(2)	C21–C20–C22	111.49(16)	C30–C31–F311	112.64(15)
F321–C32	1.452(3)	F212–C21–F213	109.99(17)	C30–C31–F312	117.46(16)
F322–C32	1.336(3)	F212–C21–F211	107.15(19)	C30–C31–F313	112.92(16)
F323–C32	1.274(3)	F213–C21–F211	104.58(19)	F311–C31–F312	108.04(16)
N1–C2	1.585(3)	C20–C22–F223	116.05(16)	F311–C31–F313	105.70(16)
N1–C6	1.395(2)	C20–C22–F221	109.34(16)	F312–C31–F313	98.67(17)
O20–C20	1.496(2)	C20–C22–F222	110.45(17)	F321–C32–F323	111.85(19)
O30–C30	1.376(2)	C20–C21–F212	117.68(18)	F322–C32–F323	109.31(19)
C2–C3	1.512(3)	C20–C21–F213	108.75(17)	F321–C32–C30	113.29(18)
C3–C4	1.417(3)	C20–C21–F211	107.87(18)	F321–C32–F322	104.62(18)
C4–C5	1.616(4)				
C5–C6	1.506(3)				
C20–C21	1.522(3)				
C20–C22	1.543(3)				
C30–C31	1.662(3)				
C30–C32	1.436(3)				

by full-matrix least-squares based on F using CRYSTALS software [15]. All non-hydrogen atoms were anisotropically refined. The hydrogen atoms were located in difference Fourier maps. H atoms were refined isotropically with $U_{iso} = 1.20U_{eq}$ where U_{eq} is the equivalent isotropic atomic displacement parameter of the attached atom. The crystal parameters, data collection and the refinement details of compound are reported in Tables 2 and 3. These data were deposited at Cambridge Crystallographic Data Centre (No. CCDC 256662).

References

[1] M.J. Kamlet, J.L.M. Abboud, M.H. Abraham, R.W. Taft, J. Org. Chem. 48 (1983) 2877–2887.

[2] J.-P. Bégué, D. Bonnet-Delpon, B. Crousse, Synlett (2004) 18–29, and references cited herein.

[3] U. Das, B. Crousse, V. Kesavan, D. Bonnet-Delpon, J.-P. Bégué, J. Org. Chem. 65 (2000) 6749–6751.

[4] (a) W.J. Middleton, R.V. Lindsey, J. Am. Chem. Soc. 86 (1964) 4948–4952;
(b) A. Berkessel, J.A. Adrio, D. Hüttenhain, J.M. Neudörfl, J. Am. Chem. Soc. 128 (2006) 8421–8426.

[5] (a) K.F. Purcell, J.A. Stikeleather, S.D. Brunk, J. Am. Chem. Soc. 91 (1969) 4019–4027;
(b) M.A. Munoz, M. Galan, C. Carmona, M. Balon, Chem. Phys. Lett. 401 (2005) 109–114;
(c) W.R. Moomaw, T.-Y. Liu, J.E. Kenny, J. Phys. Chem. 99 (1995) 7320–7323;
(d) N.C. Maiti, P.R. Carey, V.E. Anderson, J. Phys. Chem. A 107 (2003) 9910–9917;
(e) N.C. Maiti, Y. Zhu, I. Carmichael, A.S. Serianni, V.E. Anderson, J. Org. Chem. 71 (2006) 2880–5878;
(f) J. Graton, M. Berthelot, F. Besseau, C. Laurence, J. Org. Chem. 70 (2005) 7892–7901;
(g) T. Katagiri, Y. Fujiwara, S. takahashi, K. Uneyama, J. Fluorine Chem. 126 (2005) 1134–1139.

[6] (a) H. Schaal, T. Häber, M.A. Suhm, J. Phys. Chem. A 104 (2000) 265–274;
(b) M. Hyacinth, M. Chruszcz, K. Sung Lee, M. Sabat, G. Gao, L. Pu, Angew, Chem. Int. Ed. 45 (2006) 5358–5360;
(c) S. Takahashi, T. Katagiri, K. Uneyama, Chem. Commun. (2005) 3658–3660.

[7] R. Taylor, O. Kennard, Acc. Chem. Res. 17 (1984) 320–326.

[8] J. Chen, M.A. McAllister, J.K. Lee, K.N. Hook, J. Org. Chem. 63 (1998) 4611–4619.

[9] J.E. Del Bene, J.A. Pople, J. Chem. Phys. 58 (1973) 3605.

[10] (a) A. Kivinen, J. Murto, S. Liljequist, Acta Chem. Scand., Ser. A: Phys. Inorg. Chem. A29 (1975) 911;
(b) M. Plass, A. Kolbe, J. Mol. Struct. 267 (1992) 21;
(c) N.C. Maiti, P.R. Carey, V.E. Anderson, J. Phys. Chem. A 107 (2003) 9910;
(d) H. Schaal, T. Häber, M.A. Suhm, J. Phys. Chem. A 104 (2000) 265.

[11] J. Murto, A. Kivinen, R. Viitala, J. Hyömäki, Spectrochim. Acta 29A (1973) 1121.

[12] K. Yoshida, T. Yamaguchi, T. Adachi, T. Otomo, D. Matsuo, T. Takamuku, N. Nishi, J. Chem. Phys. 119 (2003) 6132.

[13] ASTRO (5.00), SAINT (5.007) and SADABS (5.007), Data Collection and Processing Software for the SMART System (5.054), Siemens (BRUKER-AXS) Analytical X-ray Instruments Inc., Madison, WI, 1998.

[14] A. Altomare, M.C. Burla, M. Camalli, G.L. Cascarano, G. Giacovazzo, A. Guagliardi, A. Grazia, G. Moliterni, G. Polidori, R. Spagna, J. Appl. Crystallogr. 32 (1999) 115.

[15] D.J. Watkin, C.K. Prout, J.R. Carruthers, P.W. Betteridge, R.I. Prout, CRYSTALS Issue 11, Chemical Crystallography Laboratory, University of Oxford, UK, 2001.

[16] D.J. Watkin, C.K. Prout, L.J. Pearce, CAMERON, Chemical Crystallography Laboratory, University of Oxford, UK, 1996.